

Intensity of the cosmic X-ray background from HEAO1/A2 experiment

M. Revnivtsev^{1,2}, M. Gilfanov^{1,2}, K. Jahoda³, and R. Sunyaev^{1,2}

¹ Max-Planck-Institute für Astrophysik, Karl-Schwarzschild-Str. 1, 85740 Garching bei München, Germany
e-mail: mikej@mpa-garching.mpg.de

² Space Research Institute, Russian Academy of Sciences, Profsoyuznaya 84/32, 117810 Moscow, Russia

³ Laboratory for High Energy Astrophysics, Code 662, Goddard Space Flight Center, Greenbelt, MD 20771, USA

Received 13 December 2004 / Accepted 4 August 2005

ABSTRACT

We reanalyze data of HEAO1/A2 – the Cosmic X-ray Experiment – in order to repeat the measurements of the cosmic X-ray background (CXB) intensity and accurately compare this value with other measurements of the CXB. We used the data of MED, HED1, and HED3 detectors in scan mode, which allowed us to measure effective solid angles and effective areas of detectors self consistently, in the same mode as the CXB intensity was measured. We found that the average value of the CXB intensity is $1.96 \pm 0.10 \times 10^{-11}$ erg s⁻¹ cm⁻² deg⁻² in the energy band 2–10 keV, or 9.7 ± 0.5 phot s⁻¹ cm⁻² at 1 keV assuming the power law spectral shape with photon index $\Gamma = 1.4$ in this energy band. We compare the obtained measurements with those obtained by different instruments over the past few decades.

Key words. cosmology: observations – X-rays: general

1. Introduction

Emission of extragalactic X-ray sources, discovered in 1962 (Giacconi et al. 1962) as the cosmic X-ray background (CXB), still remains one of the most interesting topic of X-ray astronomy and observational cosmology. Over past few decades it was shown that the cosmic X-ray background consists of emission of a large number of point sources (see e.g. Giacconi et al. 2002), mostly active galactic nuclei (AGNs). The focusing telescopes like EINSTEIN, ROSAT, CHANDRA, and XMM have resolved most of the CXB into separate point-like objects. In view of such progress in this field, special attention is now paid to the accurate measurements of the CXB intensity value. During the past decades many different instruments measured the intensity of the CXB, and yet there are still some discrepancies between the obtained values (see e.g. Moretti et al. 2003; Revnivtsev et al. 2003 and references therein).

Probably the most important information about the shape and the average amplitude of the CXB in X-ray energy range (~2–60 keV) is still based on the measurements of HEAO1 observatory (1977–1979). The instrument Cosmic X-ray Experiment (also known as A-2 experiment) onboard this observatory was specially designed for accurate measurements of the CXB. The key feature of this instrument was the ability to distinguish between the internal instrumental background and cosmic X-ray background (see e.g. Rothschild et al. 1979; Marshall et al. 1980; Boldt 1987). The HEAO1 observatory spent a significant fraction of its lifetime scanning the

whole sky, which allowed all sky survey to be constructed (e.g. Piccinotti et al. 1982; Wood et al. 1984; Levine et al. 1984) and the cosmic X-ray background to be measured over a very wide sky solid angle (e.g. Marshall et al. 1980; Boldt 1987; Gruber et al. 1999).

One of the main difficulties in the comparison of the CXB results of different observatories is the accuracy of their cross-calibrations. Proportional counters with collimators, which have given a lot of information about the CXB, are relatively easy to crosscalibrate if they work in similar energy bands. Ability to observe the Crab nebula, which is now considered an almost perfectly stable celestial source, allows one to use this source for straightforward crosscalibration of the instruments. Unfortunately, published information about the parameters of HEAO1/A2 detectors is not sufficient for accurate crosscalibration of its results with results obtained by modern satellites.

In this paper we reanalyze data of HEAO1/A2 experiment and obtain the intensity of the CXB and important instrumental parameters of HEAO1/A2, which allowed us to compare the results of HEAO1/A2 relatively accurately with those of other instruments.

2. HEAO1/A-2 instrument

A detailed description of the Cosmic X-ray Experiment (A2) onboard HEAO1 observatory can be found in Rothschild et al. (1979). Here we only briefly describe the general features of the instrument.

The A2 experiment (Cosmic X-ray Experiment) of HEAO1 observatory consisted of three sets of different types of detectors. All detectors were proportional counters with different filling gas. Low Energy Detectors (LED) worked in the energy band 0.15–3 keV; Medium Energy Detector (MED) had the effective energy band 1.5–20 keV, and High Energy Detectors (HED) had the energy band 2–60 keV.

The biggest advantage of the A2 was the ability to separate the internal instrumental background from the cosmic X-ray background. This was achieved by a special design of detectors. All 6 detectors of the A2 were proportional counters with detective layers of anodes. Half of the anodes were illuminated through $\sim 3^\circ \times 3^\circ$ collimators, and another half through $\sim 1.5^\circ \times 3^\circ$ (or $\sim 6^\circ \times 3^\circ$) collimators. The flux of the cosmic X-ray background measured by detectors rises with their collimator's solid angles. On the other hand, the instrumental background in the different parts of the detectors that were under different collimators was the same by design; two types of collimators were interlaced with each other and detecting anodes under them were intermixed (see a more detailed description in Rothschild et al. 1979). The total flux, detected by different halves of the detectors, which see the sky through different collimators: $C_L = C_{\text{bkg}} + C_{\text{CXB,L}}$, $C_S = C_{\text{bkg}} + C_{\text{CXB,S}}$. Here C_{bkg} is count rate of the internal background, and C_{CXB} is count rate produced by the cosmic X-ray background in the large (L) and small (S) fields of view parts of the detector. Keeping in mind that the internal background is the same for L and S parts of the detector, the CXB flux detected by the “small” half of the detector ($C_{\text{CXB,S}}$) can be calculated from the simple formula:

$$C_{\text{CXB,S}} = (C_L - C_S) \left(\frac{A_L \Omega_L}{A_S \Omega_S} - 1 \right)^{-1} \text{ cnts/s} \quad (1)$$

in which $A\Omega$ is the production of effective area and solid angle of the L and S parts of the detector.

3. Data analysis

One of the main goals of the HEAO1/A2 experiment was to measure the intensity of the CXB averaged over a large sky solid angle. For this purpose, the satellite rotated around the Sun-pointed axis (33 min period), which was gradually stepped every 12 h by $\sim 0.5^\circ$, in order to remain pointed at the Sun. The measurement of the CXB was based on formula (1) (see Marshall et al. 1980).

During the scanning mode, the HEAO1/A2 covered the whole sky (Piccinotti et al. 1982) including the Crab nebula. This gives us an opportunity to use the measurements of the Crab nebula for accurate crosscalibration with other collimated instruments. Assuming the same photon flux of the Crab nebula for all instruments, we can rescale their effective area (if needed); and using the scans of the HEAO1/A2 detectors over the source, we can determine the collimator's effective solid angles.

For our analysis we used the HEAO1/A2 database in Goddard Space Flight Center (ftp://heasarc.gsfc.nasa.gov/FTP/hea01/data/a2/xrate_fits). The database provides the count rate measurement of all A2 detectors every 1.28 s. The count rate measurements are presented

in the form of discovery scalars, i.e. count rates of detectors in certain energy bands (for more detailed description see Marshall 1983; Allen et al. 1994) Definition of some discovery scalars changed throughout the mission. Therefore for our purpose, we used only those scalars which have not been changed, that is the total count rate of different parts of different anode layers of the detectors: 1L, 1R, 2L and 2R. Here L and R denote so-called “left” and “right” parts of the detectors, placed under different size collimators (see Rothschild et al. 1979).

We used only data from the detectors MED, HED1, and HED3 for the following reasons. As we are interested here in the hard X-ray background (>2 keV), we do not consider here LED detectors which worked in 0.15–3 keV energy band. We also do not consider data of detector HED2, which lacks the particle veto layer.

The data were selected using the following criteria:

1. We analyzed only data obtained during scan mode. For the HED3 detector, we used only data before day 304 of the mission, for which period we have the response matrices of two separate layers of the the detector.
2. Data is “clean”, i.e. detector's fields of view exclude the Earth plus its 100 km atmosphere; high voltage is on and stable; the calibration rods are outside the MED field of view.
3. Electron contamination is not important.

For subsequent analysis of the obtained count rate values, we used response matrices of A2 provided by the HEASARC archive (<http://heasarc.gsfc.nasa.gov/FTP/hea01/data/a2/responses/>).

For determination of the collimator's solid angles and effective areas of the A2 detectors, we used data of scans over the Crab nebula. The A2 collimators are made of rectangular cross section tubes, therefore providing roughly linear dependence of the effective area of a detector on the source offset within the field of view.

$$C = CR \left[1 - \frac{\phi}{\phi_0} \right] \left[1 - \frac{\theta}{\theta_0} \right] \quad (2)$$

here C is the measured Crab nebula count rate at certain offset ϕ, θ ; CR is the Crab nebula count rate observed by the detector at zero offset, ϕ_0 and θ_0 are sizes of the collimator field of view across the scan plane (approximately $\sim 3^\circ$) and along the scan plane ($\sim 1.5^\circ, 3^\circ$, or 6°). The shape of the collimator off-axis response function is shown in Fig. 1. Fluxes of the Crab nebula measured by each A2 detector at different offsets provide the shape of the collimator response function. We fitted the measured values by the described model (see formula (2)) using standard χ^2 minimization technique. The quality of the fit in all cases is good and the ratio of χ^2 to the number of degrees of freedom never exceeds 1.2. Best fit parameters of the model are presented in Table 1.

In order to convert the observed maximal Crab count rate (CR) into the effective area of the detectors (with the help of known response matrices), we assumed that the Crab spectrum is a power law ($dN/dE = AE^{-\Gamma}$) with $\Gamma = 2.05$ and that the normalization at 1 keV $A = 10 \text{ phots}^{-1} \text{ cm}^{-2} \text{ keV}^{-1}$

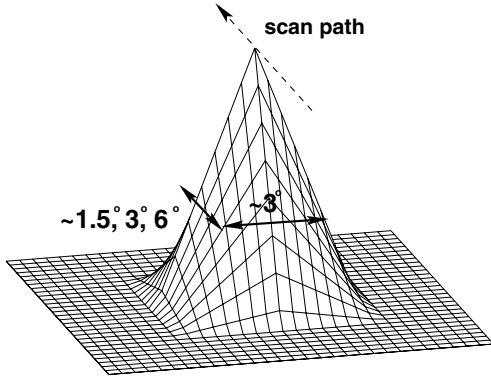


Fig. 1. Dependence of the effective area of HEAO1 detectors on the offset position of a source in the field of view. In the direction along the scan path collimators had $FWHM \sim 1.5^\circ$, $\sim 3^\circ$ and $\sim 6^\circ$ size. Perpendicular to the scan path the size of all collimators had $FWHM \sim 3^\circ$.

(Seward 1978; Zombeck 1990), similar to the one used in Revnivtsev et al. (2003). The energy flux of the Crab in this case equals $2.39 \times 10^{-8} \text{ erg s}^{-1} \text{ cm}^{-2}$ in the energy band 2–10 keV. The obtained (measured) Crab count rate (CR in formula (2)) depends on the response matrix of the detector, which we took from HEASARC HEAO1 archive (see reference above) and its effective area. In Table 1 we present the best fit parameters of A2 MED, HED 1, and HED3 detectors.

The uncertainties of these values have two main origins. The statistical uncertainties are rather small. Typically they are not higher than $\sim 1\%$. The angular sizes of collimators and the effective solid angle can be determined with accuracy of $\sim 1\%$. However, the values of effective areas of the detectors strongly depend on the assumed spectrum of the Crab nebula and the accuracy of the used response matrices. For example, the difference around 0.05 in the photon index Γ of the Crab nebula (leaving energy flux of the Crab in the energy band 2–10 keV unchanged) will change the count rate to an energy flux conversion factor by a 1–2% for MED detectors and 2–3% for HED detectors. The difference in the assumed Crab nebula flux linearly translates into the changes of effective area values.

4. Results

The main idea of measuring the intensity of the CXB with the help of the HEAO1/A2 instrument is to use the fact that the flux of the CXB linearly scales with the solid angle of the detectors. The design of the A2 detectors allowed us to exclude the instrumental background with almost absolute accuracy (see details in Rothschild et al. 1979; Boldt 1987). By measuring the average level of the difference between count rates of large and small solid angle detectors, we can calculate the intensity of the CXB using formula (1). Coefficients $A_L \Omega_L / (A_S \Omega_S)$ can be calculated from Table 1.

For measuring the flux difference between the large and the small solid angle detectors we have used data from a part of the sky with galactic latitudes $|b| > 20^\circ$, and also we excluded a region around the very bright Galactic X-ray source Sco X-1 (10° around Sco X-1). After this procedure, some galactic sources still remain on the sky (e.g. Her X-1); however they

Table 1. Parameters of detectors of A2, determined from the scanning observations.

	ϕ_0 , deg	θ_0 , deg	Ω , deg ²	CR ^a	A_{eff} , cm ²
MED					
layer1, left	2.88	2.93	8.44	602	405
layer1, right	2.92	1.42	4.15	539	362
layer2, left	2.86	2.93	8.38	269	366
layer2, right	2.90	1.43	4.09	243	331
HED1					
layer1, left	3.15	2.84	8.95	559	335
layer1, right	3.15	5.87	18.49	564	338
layer2, left	3.16	2.88	9.10	55.6	331
layer2, right	3.13	5.86	18.34	55.4	324
HED3					
layer1, left	3.10	2.96	9.17	607	354
layer1, right	3.09	1.48	4.56	577	336
layer2, left	3.05	2.89	8.81	58.5	340
layer2, right	3.04	1.49	4.53	53.7	313

^a Crab count rate in the detectors, cnts/s.

All effective areas were calculated using the response matrices from the HEAO1/A2 archive in GSFC; namely, m11n.rsp and m12n.rsp for two layers of MED, h111095c.rsp and h121095c.rsp for HED1, h31257c.rsp and h321095c.rsp for HED3 detectors.

contribute less than 1% to the total sky flux. Point-like extragalactic sources which can be detected from HEAO1/A2 survey (the flux is higher than $\sim 3 \times 10^{-11} \text{ erg s}^{-1} \text{ cm}^{-2}$, see Piccinotti et al. 1982) are part of the cosmic X-ray background, but in any case they do not contribute more than ~ 1 –2% to the total CXB flux from the whole sky. Therefore we did not exclude them from our analysis.

The measured averaged difference between the large and the small solid angle parts of layer 1 MED detector equals $C_L - C_S = 2.23 \text{ cnts/s}$. Therefore $C_{\text{CXB,S}} = 1.75 \text{ cnts/s}$. In order to convert this count rate into the physical units ($\text{erg s}^{-1} \text{ cm}^{-2} \text{ FOV}^{-1}$), we should assume the shape of the CXB spectrum. The best measurement of the CXB spectrum in such a broad energy range (2–60 keV in our case) was done by Marshall et al. (1980). The CXB spectrum was empirically described by a thermal bremsstrahlung model with the temperature $kT = 40 \text{ keV}$. Below we will always assume this shape of the CXB spectrum for our analysis.

Using this shape of the CXB spectrum and the response matrix of the layer 1 MED detector, we can convert the observed count rate into the CXB intensity in the energy range 2–10 keV $I_{\text{CXB}} = 8.92 \times 10^{-11} \text{ erg s}^{-1} \text{ cm}^{-2} \text{ FOV}^{-1}$. The effective solid angle of the small FOV of MED(layer1) is 4.15 deg^2 , which gives the estimation of the CXB intensity from the first layer of MED $I_{\text{CXB,MED,M1}} = 2.15 \times 10^{-11} \text{ erg s}^{-1} \text{ cm}^{-2} \text{ deg}^{-2}$.

The same set of calculations gave for the second layer of MED: $I_{\text{CXB,MED,M2}} = 1.97 \times 10^{-11} \text{ erg s}^{-1} \text{ cm}^{-2} \text{ deg}^{-2}$. Similar calculations for HED detectors give values presented in Table 2.

Table 2. Values of the CXB intensity in the energy band 2–10 keV, obtained from different layers of different detectors of HEAO1/A2.

	MED	HED1	HED3
Layer1	2.15	1.82	1.98
Layer2	1.97	1.90	1.91

All values in the units of 10^{-11} erg s $^{-1}$ cm $^{-2}$ deg $^{-2}$.

5. Discussion

Accurate measurements of the CXB intensity are quite complicated. The main problems can be divided into three parts: 1) subtraction of the internal instrumental background, 2) accurate measurement of the effective solid angle of the instrument (including the so-called stray light contribution to the count rate detected by X-ray telescopes), and 3) accurate measurement of the instrument effective area and its dependence on energy.

In our approach, we accurately determined solid angles of the detectors using the celestial calibration source (Crab nebula) and accurately subtracted the instrumental background, because of the special design of the instrument. Stating that the Crab nebula spectrum have the adopted shape ($dN/dE = 10E^{-2.05}$ phot s $^{-1}$ cm $^{-2}$ keV $^{-1}$) in the energy range 2–60 keV, the uncertainties of the obtained effective area values only depend on the knowledge of the detector's response functions.

We have 6 independent measurements of the CXB using MED, HED1, and HED3 detectors and can try to estimate total uncertainty of the obtained CXB intensity by calculating the rms deviation of the individual measurements from the average one. We then obtain CXB intensity $I_{\text{CXB}} = 1.96 \pm 0.10$ erg s $^{-1}$ cm $^{-2}$ deg $^{-2}$.

5.1. Comparison with collimated experiments

First generations of X-ray instruments, which was represented mainly by collimated spectrometers, could overcome problems number (2) and (3). Comparison of the Crab nebula count rates, whose spectrum and flux are considered stable, can provide us with an accurate crosscalibration, if we know the response function of the instrument, even without accurate knowledge of the instrument effective area. The effective solid angle of the collimator can also be measured directly from observations and compared to that of other instruments.

In view of such simplification, it is interesting to compare the measurements of the CXB intensity made by collimated spectrometers. We combined the values of CXB intensity measured by these experiments (rockets in Gorenstein et al. 1969; Palmieri et al. 1971; McCammon et al. 1983; HEAO1 in this work; RXTE/PCA in Revnivtsev et al. 2003) in Table 3 along with their claimed Crab nebula fluxes. The flux of the Crab nebula presented in these works can be used in order to recalculate the effective areas of the instruments. In order to obtain corrected CXB intensity value, we divided the CXB intensity value provided by authors by the ratio of their Crab nebula flux in 2–10 keV energy band to 2.39×10^{-8} erg s $^{-1}$ cm $^{-2}$, which we adopted here. The corrected values of the CXB intensity (Table 3) we obtain are remarkably consistent with each other.

Table 3. Summary of measurements of the CXB intensity with different observatories. CXB $_{\text{corr}}$ is the CXB intensity corrected for rescaling factors between observatories (see text)

Instrument	Ref.	CXB	Crab	CXB $_{\text{corr}}$
Rockets	1	1.57 ± 0.15	2.27	1.65 ± 0.16
Rockets	2	1.90 ± 0.20	–	–
Rockets	3	2.20 ± 0.20	2.29	2.29 ± 0.21
HEAO/A2	4	1.96 ± 0.10	2.39	1.96 ± 0.10
RXTE/PCA	5	1.94 ± 0.19	2.39	1.94 ± 0.19
ASCA/GIS	6	1.94 ± 0.19	2.16	2.14 ± 0.21
BeppoSAX	7	2.35 ± 0.12	2.01	2.79 ± 0.14
XMM/EPIC-PN	8	2.15 ± 0.16	– ^a	2.51 ± 0.30
XMM/EPIC-PN	9	2.24 ± 0.16	– ^a	2.62 ± 0.18

CXB intensity is expressed in units 10^{-11} erg s $^{-1}$ cm $^{-2}$ deg $^{-2}$, and the Crab nebula flux is in units 10^{-8} erg s $^{-1}$ cm $^{-2}$. Energy band 2–10 keV. References: 1 – Gorenstein et al. (1969), 2 – Palmieri et al. (1971), 3 – McCammon et al. (1983), 4 – this work, 5 – Revnivtsev et al. (2003), 6 – Kushino et al. (2002), 7 – Vecchi et al. (1999), 8 – Lumb et al. (2002), 9 – De Luca & Molendi (2004).

^a Rescaling was done using observations of 3C 273, see text.

The deviation of the values does not exceed 2σ level. It is important to note here that uncertainties of the effective solid angles of rocket flight experiments might lead to another correction, which is not possible for us to do here.

A relatively big difference between the CXB intensity value presented in the original work on HEAO1/A2 data ($I_{\text{CXB}} \sim (1.67 \pm 0.17) \times 10^{-11}$ erg s $^{-1}$ cm $^{-2}$ deg $^{-2}$) and the result presented in this paper is most likely caused by different assumptions on the normalization of the Crab nebula spectrum. Unfortunately in the original work of Marshall et al. (1980), information about this normalization factor is absent.

5.2. Comparison with focusing telescopes

Over past few decades a number of measurements of the CXB intensity were made with the help of focusing telescopes. In Table 3 we summarize the CXB intensity values obtained by ASCA, BeppoSAX, and XMM-Newton observatories.

Crosscalibration of effective areas of the ASCA and BeppoSAX instruments with those of the collimated experiments can be done with the help of the Crab nebula. We should remember that, after this cross check, there are still uncertainties in the effective solid angles of focusing telescopes, which cannot be overcome by comparison of the Crab nebula fluxes.

Crosscalibration of the XMM-Newton instruments with the collimated spectrometers and with ASCA and BeppoSAX is less clear, because it cannot be done via measurements of the Crab nebula. However, for such purposes, one can use strictly simultaneous observations of weak pointlike objects. For example, we can use simultaneous XMM and RXTE observations of the quasar 3C273 (Courvoisier et al. 2003). The rescaling factor, determined in the paper of Courvoisier et al. (2003), cannot be used by us here because the flux of the Crab nebula assumed by the authors (which is build-in

the LHEASOFT 5.2 package tasks used in that paper) was higher than the value assumed by us (see discussion of this topic in Revnivtsev et al. 2003). Our estimate of the RXTE/PCA-XMM/EPIC_PN rescaling factor is 1.17 ± 0.10 , i.e. the PCA flux of a source is $17 \pm 10\%$ higher than that of EPIC-PN.

Considering the above mentioned numbers with quoted uncertainties, we can conclude that there are some indications that the intensity of the CXB measured by focusing telescopes is higher than that measured by collimated experiments. Such discrepancy is now limited to $\sim 10\text{--}15\%$ and practically does not exceed the 2σ confidence limits of individual measurements. The nature of this discrepancy is still unknown. One possible reason can be the extreme complexity measuring effective solid angles (stray light effects) of focusing telescopes in comparison with those of collimated experiments.

Acknowledgements. M.R. thanks Pavel Shtykovskiy for his help with XMM data analysis. We thank the anonymous referee, who helped us to significantly improve the paper. This research made use of data obtained through the High Energy Astrophysics Science Archive Research Center Online Service, provided by the NASA/Goddard Space Flight Center.

References

- Allen, J., Jahoda, K., & Whitlock, L. 1994, HEAO-1 and the A2 experiment, *Legacy*, 5
- Boldt, E. 1987, *Phys. Rep.*, 146, 215
- De Luca, A., & Molendi, S. 2004, *A&A*, 419, 837
- Giacconi, R., Gursky, H., Paolini, R., & Rossi, B. 1962, *Phys. Rev. Lett.*, 9, 439
- Giacconi, R., Zirm, A., Wang, J., et al. 2002, *ApJS*, 139, 369
- Gorenstein, P., Kellogg, E. M., & Gursky, H. 1969, *ApJ*, 156, 315
- Gruber, D. E., Matteson, J. L., Peterson, L. E., & Jung, G. V. 1999, *ApJ*, 520, 124
- Kushino, A., Ishisaki, Y., Morita, U., et al. 2002, *PASJ*, 54, 327
- Levine, A. M., Lang, F. L., Lewin, W. H. G., et al. 1984, *ApJS*, 54, 581
- Lumb, D. H., Warwick, R. S., Page, M., & De Luca, A. 2002, *A&A*, 389, 93
- McCammon, D., Burrows, D., Sanders, W., & Kraushaar, W. 1983, *ApJ*, 269, 107
- Marshall, F., Boldt, E., Holt, S., et al. 1980, *ApJ*, 235, 4
- Marshall, F. E. 1983, HEAO 1 A-2 Experiment: The Configuration of the Hard X-ray Detectors, GSFC preprint
- Moretti, A., Campana, S., Lazzati, D., & Tagliaferri, G. 2003, *ApJ*, 588, 696
- Palmieri, T. M., Burginyon, G. A., Grader, et al. 1971, *ApJ*, 169, 33
- Piccinotti, G., Mushotzky, R. F., Boldt, E. A., et al. 1982, *ApJ*, 253, 485
- Rothschild, R., Boldt, E., Holt, S., et al. 1979, *Space Sci. Instr.*, 4, 269
- Revnivtsev, M., Gilfanov, M., Jahoda, K., & Markwardt, C. 2003, *A&A*, 411, 329
- Seward, F. 1978, *Journal of the British Interplanetary Society*, 31, 83
- Courvoisier, T. J.-L., Beckmann, V., Bourban, G., et al. 2003, *A&A*, 411, 343L
- Vecchi, A., Molendi, S., Guainazzi, M., et al. 1999, *A&A*, 349, L73
- Wood, K. S., Meekins, J. E., Yentis, D. J., et al. 1984, *ApJS*, 56, 507
- Zombeck, M. V. 1990, *Handbook of Astronomy and Astrophysics*, Second Edition (Cambridge, UK: Cambridge University Press)